

Synthesis and characterization of tin oxide-modified mesoporous SBA-15 molecular sieves and catalytic activity in trans-esterification reaction

Pallavi Shah^a, Arumugamangalam V. Ramaswamy^b, Karoly Lazar^c,
Veda Ramaswamy^{a,*}

^aCatalysis Division, National Chemical Laboratory, Pune 411008, India

^bChemistry Department, University of Pune, Pune 411007, India

^cInstitute of Isotope and Surface Chemistry, CRC, HAS, P.O. Box 77, Budapest H-1525, Hungary

Received in revised form 16 June 2004; accepted 21 June 2004

Available online 4 August 2004

Abstract

Mesoporous silica molecular sieve SBA-15 has been synthesized and incorporated with various amounts of tin via incipient-wetness impregnation using tin chloride in ethanol followed by calcination. Characterization was done by X-ray fluorescence spectrophotometry (XRF), powder X-ray diffraction (PXRD), nitrogen adsorption, diffuse reflectance ultraviolet (DRUV), scanning and transmission electron microscopy (SEM, TEM), FTIR, ²⁹Si and ¹¹⁹Sn MAS NMR, and Sn-Mössbauer spectroscopic techniques to understand the chemical nature of incorporated tin. The silanol groups on the internal walls of SBA-15 are suggested to be the sites for tin incorporation. Bulk structural characterization techniques (X-ray diffraction and BET) are used to demonstrate that the hexagonal structure is maintained during impregnation. Tin oxide exists as a thin film anchored inside the mesopores of SBA-15. Complementarily, ¹¹⁹Sn NMR and Mössbauer spectroscopies are used to investigate the microstructure of the Sn centers grafted to the mesoporous walls. Sn-Mössbauer spectroscopic studies reveal that Sn²⁺ may form upon reductive treatments and can probably be stabilized atomically in the pore wall, whereas Sn⁴⁺ is stabilized as large entities. While SBA-15 itself shows some activity in transesterification of diethyl malonate with various alcohols, Sn-SBA-15 samples are found to possess enhanced catalytic activity for the same.

© 2004 Elsevier B.V. All rights reserved.

Keywords: SBA-15; SnO₂; Sn-SBA-15; Transesterification

1. Introduction

Many researchers have reported the potential applications of mesoporous materials having uniform pore structure and an extensively high surface area as catalysts, adsorbents for large organic molecules and guest–host chemical supports [1–4]. Compared to the crystalline microporous materials, the mesoporous materials suffer two major disadvantages: i.e., low intrinsic catalytic activity due to the amorphous nature of the pore walls and poor hydrothermal and mechanical stability due to the high hydrophilicity derived from abundant silanol groups [5]. The stability of the mesoporous

materials has been improved through (a) controlled synthesis conditions in order to achieve extensive condensation of the silica walls, (b) by post-modification and (c) by discovering new materials that are intrinsically stable. SBA-15 is a mesoporous silica molecular sieve with uniform channels varying from 50 to 300 Å, synthesized with triblock copolymers having thicker walls, and hence a higher hydrothermal stability than conventional MCM-41 [6,7]. Several reports on the incorporation of Al [8,9], Ti [10,11] or V [12] into SBA-15 have appeared recently. The post-synthesis method is still overwhelmingly used, mainly because SBA-15 needs strongly acidic synthesis conditions. In the present work, we report on the synthesis of SBA-15 with an aim to introduce Sn in different concentrations to obtain thin SnO₂ molecular films anchored inside the mesopores of

* Corresponding author. Tel.: +91 20 2589 3761; fax: +91 20 2589 3761.

E-mail address: veda@cata.ncl.res.in (V. Ramaswamy).

SBA-15. The samples were characterized by a variety of techniques to understand the location and environment of Sn in Sn-SBA-15.

Esterification of carboxylic acids and transesterification of esters have wide academic as well as industrial importance. A number of useful esterification methods have been reported in the literature, catalyzed by a variety of acids, ion exchange resins, zeolites, and solid acid catalysts [13–22]. Transesterifications are catalyzed by alkali metal hydroxides, alkoxides and tin, calcium or titanium compounds [23]. Environmental considerations limit the applicability of many homogeneous and heterogeneous catalysts, because of the problem of separation and reusability of the catalysts. Few reagents are available for commercial applications that can accomplish both esterification and transesterification reactions under mild conditions. Recent methods are those using diphenyl ammonium triflate or a clay catalyst [24]. Reagents based on iodine reported in recent years for transesterification reactions include indium triiodide, [25] iodotrimethyl silane–iodine, [26] and others. Recently, transesterification has become important in producing biodiesel. Tin is already known to catalyze transesterification reactions [27]. In the present study, we report on the catalytic activity of SBA-15 and Sn-SBA-15 samples for transesterification of diethylmalonate (DEM) with various alcohols.

2. Experimental section

2.1. Catalyst preparation

Mesoporous silica SBA-15 was synthesized according to the reported procedure [6,7]. In a typical synthesis, 2 g of amphiphilic triblock copolymer, poly (ethylene glycol)-block-poly (propylene glycol)-block-poly (ethylene glycol) [average molecular weight 5800, Aldrich], was dispersed in 15 g of water and 60 g of 2 M HCl solution while stirring, followed by the addition of 4.25 g of tetraethyl orthosilicate (Aldrich) to the homogeneous solution. This gel was continuously stirred at 313 K for 24 h, and finally crystallized in a Teflon-lined autoclave at 373 K for 2 days. After crystallization, the solid product was centrifuged, filtered, washed with deionized water, and dried in air at room temperature. The material was calcined in air at 823 K for 24 h to decompose the triblock copolymer and to obtain a white powder (SBA-15).

Tin oxide-modified SBA-15 was prepared by the incipient-wetness impregnation method [28] under nitrogen atmosphere. Mesoporous silica SBA-15 was placed in a round-bottom flask and a solution of $\text{SnCl}_4 \cdot 5\text{H}_2\text{O}$ in ethanol was added to it. Varying amounts of $\text{SnCl}_4 \cdot 5\text{H}_2\text{O}$ (corresponding to Si/Sn = 5–80) were dissolved in 10 ml of ethanol for each 0.5 g of SBA-15. The material was stirred at room temperature under nitrogen atmosphere for 24 h and then calcined in air at 823 K for 6 h to obtain tin oxide-modified mesoporous

silica. The samples are designated with values in parentheses, which refer to initial Si/Sn ratios of the samples.

2.2. Catalyst characterization

The content of tin oxide in Sn-SBA-15 was estimated using a X-ray fluorescence spectrophotometer, Rigaku 3070E, with a Rh target. The powder XRD patterns of calcined sample were taken from an X'Pert Pro (Philips) diffractometer using $\text{Cu K}\alpha$ radiation and a proportional counter as detector. A divergent slit of $1/32^\circ$ on the primary optics and an anti-scatter slit of $1/16^\circ$ on the secondary optics were employed to measure the data in the low angle region. Scanning electron micrographs of the samples were recorded on a JEOL-JSM-5200 SEM to observe the morphology of the particles. TEM of the samples were recorded on a JEOL Model 1200EX microscope operating at 100 kV. A calcined sample was dispersed in isopropyl alcohol, deposited on a Cu grid and dried. The BET surface area of the samples was determined by N_2 adsorption at 77 K by using NOVA 1200 (Quanta Chrome) equipment. Prior to N_2 adsorption, the samples were evacuated at 573 K. The specific surface area, S_{BET} , was determined from the linear part of the BET equation ($p/p_0 = 0.05\text{--}0.31$). The pore size distribution was calculated using the Barrett–Joyner–Halenda (BJH) method.

The UV–vis diffuse reflectance spectra of the samples were obtained on a Shimadzu UV–vis spectrophotometer (UV-2500 PC). The framework IR spectra of the samples were recorded in Nujol mull in the mid framework region ($1100\text{--}400\text{ cm}^{-1}$) with a Shimadzu model 8300 FTIR spectrometer. The FTIR measurements (Nicolet 60 SXB) were carried out by using a self-supported wafer under vacuum at 673 K to study the hydroxyl region. The NMR spectroscopic studies were carried out on an AVANCE 500 MHz (BRUKER) NMR spectrometer. The resonance frequencies of ^{119}Sn , ^{29}Si were 111.8, and 59.6 MHz, respectively. The ^{119}Sn signals were referred to the isotropic peak of SnO_2 taken as $\delta = -604$ ppm (with respect to tetramethyl tin). Tetraethyl orthosilicate ($\delta = 82.4$ ppm from TMS) was used as the reference for ^{29}Si .

^{119}Sn Mössbauer spectra were recorded in an in situ cell at 77 and 300 K. Reduction treatment (for Si/Sn = 5–40) was carried out at 670 K for 2 h in CO and H_2 flow. Spectra were collected in constant acceleration mode. The positional parameters are relative to SnO_2 , their estimated accuracy being ± 0.03 mm/s. Spectra are decomposed to Lorentzian-shape lines. Temperature programmed desorption of ammonia was carried out over Micromeritics Autochem 2910 instrument. The Sn-SBA-15 sample was subjected to ammonia adsorption followed by desorption as per the following procedure. About 0.5 g of the sample was placed in a quartz reactor and activated at 773 K for 2 h under helium flow (20 ml/min). The reactor was then cooled to 353 K and 10% NH_3 in He was passed through the sample (30 ml/min) at this temperature for 30 min. The temperature was raised to

373 K and maintained for 1 h under helium flow (30 ml/min). Finally, the desorption of ammonia was carried out in a flow of helium at a heating rate of 10 K min⁻¹. The amount of ammonia desorbed from the catalyst was estimated by a TCD close to the reactor outlet.

2.3. Catalytic activity

Transesterification reactions were performed in a glass batch reactor fitted with a water-cooled condenser. The reaction was performed on a standard substrate, namely diethylmalonate with various alcohols. A mixture of diethylmalonate (0.8 g, 5 mmol), alcohols (15 mmol) and the catalyst (130 mg) was stirred at a desired temperature (383 K) for 24 h. The progress of the reaction was monitored by withdrawing aliquots of the reaction mixture and analyzing the same with a GC equipped with a FID (Agilent Technologies, model 6890 N, capillary column HP-5, 30 m, containing 5% phenyl methyl siloxane). Under optimized conditions of temperature (383 K), substrate to alcohol molar ratio (1:3) and reaction time (24 h), transesterification of diethyl malonate has been performed by various alcohols. The catalyst was recycled in some cases to check its reusability.

3. Results and discussion

The chemical composition (Si/Sn ratios) of the samples is given in Table 1. Powder XRD patterns of SBA-15 and Sn-SBA-15 (5) are shown in Fig. 1A. They exhibit very similar patterns with well-resolved diffraction peaks at 0.8° (2 θ) and two weak peaks at 1.6 and 1.7° (2 θ) due to 100, 110 and 200 Bragg reflections, respectively. This indicates a good mesoscopic order and the characteristic hexagonal features of SBA-15 are maintained in Sn-SBA-15 samples. Calcination does not alter the XRD patterns. Typical XRD data in the high angle region for the sample having Si/Sn = 5 is shown in Fig. 1B. The powder X-ray diffraction pattern confirms the presence of SnO₂ in rutile structure (tetragonal system). The 110, 101 and 211 reflections of SnO₂ can be clearly seen at 2 θ = 26.58°, 34.0° and 51.72°, respectively. The broad nature of the peaks indicates the presence of very small crystallites of SnO₂.

N₂ adsorption isotherms of calcined SBA-15 and Sn-SBA-15 with varying amounts of tin loading were recorded.

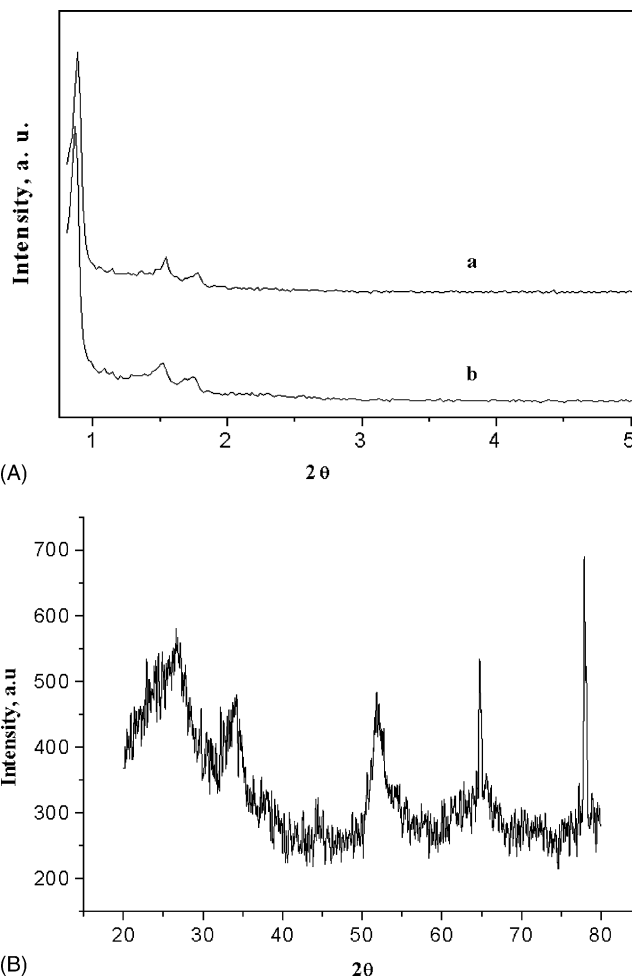


Fig. 1. (A) Powder X-ray diffraction patterns of (a) SBA-15 and (b) Sn-SBA-15 (5) samples in the region 0–5° 2 θ . (B) Powder X-ray diffraction patterns of Sn-SBA-15 (5) sample in the region 20–80° 2 θ .

A typical irreversible-type IV adsorption isotherm with H1 hysteresis loop as defined by IUPAC is observed. With increasing Sn loading, the samples give isotherms with similar inflection that shift to lower p/p_0 values (Fig. 2). The hysteresis loop is a typical feature of mesoporous materials. An increase in the N₂ adsorption amount due to multilayer adsorption was observed at higher-pressure region as SBA-15 has a larger pore size than that of MCM-41 [29–30]. The average diameters of primary mesopores, labeled as D_{BJH}, were obtained from the maximum of a pore size distribution calculated using the BJH method

Table 1
Composition and Physicochemical Characteristics of SBA-15 and Sn-SBA-15 samples

Si/Sn	XRF Si/Sn	S _{BET} (m ² g ⁻¹)	Mesopore S.A (m ² g ⁻¹)	Pore Vol. cm ³ g ⁻¹	Micropore Vol. cm ³ g ⁻¹	Pore diameter D _{BJH} (nm)	Wall thick- ness (nm)
∞	-	834	540	1.46	0.152	7.0	4.6
80	86	709	501	1.24	0.105	7.0	4.7
40	68	670	476	1.16	0.08	6.9	4.8
20	35	609	461	1.03	0.06	6.8	4.9
5	31	572	400	0.97	0.07	6.8	5.0

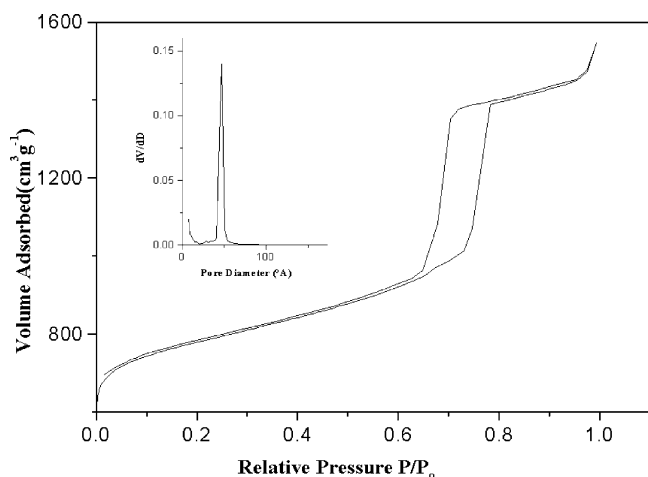


Fig. 2. N_2 adsorption/desorption isotherms of SBA-15. Inset shows the pore size distribution.

applied to the desorption part of the isotherm (Table 1). The specific surface area and the average pore size decreased after tin loading. Siliceous SBA-15 possesses a narrow pore size distribution and a high mesoporous surface area with considerable micropores, as seen from the t -plot [31–36] (Table 1). Impregnation of tin reduces the surface area. The t -plot analysis was used to estimate the micropore volume in SBA-15. We observed a gradual disappearance of the micropores on incorporation of Sn in SBA-15. Combining this with the above BET analysis, we presume that the decrease in the surface area during tin addition is essentially due to the loss of micropores. Since the micropores are probably generated by penetration of hydrophilic poly (ethylene oxide) chains of triblock copolymer into its thick silica walls, hydrothermal heating would shrink the silica walls to mend the “holes” therein, which are micropores [31–36]. Incorporation of Sn species into the micropores to remove this wall defect accounts for the reduced surface area.

Scanning electron micrographs of the SBA-15 (Fig. 3a and b) show many rope-like domains that aggregate into a wheat-like microstructure. Tin-incorporated samples show similar particle morphology.

Transmission electron micrographs of SBA-15 and Sn-SBA-15 (Fig. 4a–c) show the hexagonal array of uniform channels. A well-ordered hexagonal array of mesopores is observed, when the electron beam is parallel to the main axis of these cylinders (Fig. 4b). The two-dimensional hexagonal structure ($p6mm$) is therefore confirmed. Tin nanoparticles appear as dark objects between the walls in Fig. 4c in the sample with Si/Sn = 5. According to typical TEM images, one can estimate the pore diameter to be 6–7 nm.

Diffuse reflectance UV–vis spectroscopy was used to characterize the chemical nature and coordination states of the Sn species in the samples. The Sn-SBA-15 sample shows an absorbance band at ~ 243 nm, which can be assigned to hexacoordinated nanosized Sn species. A blue shift can be observed in the samples with increasing tin loading. An increase in the intensity of the absorption band with increase in tin content corresponds to the presence of Sn^{4+} in octahedral coordination [37,38]. The observed blue shift indicates the appearance of quantum-sized effects, well known in nano-sized semiconductor particles or thin films.

The IR spectra of the SBA-15 and Sn-SBA-15 samples are presented in Fig. 5. The IR spectra of both SBA-15 and Sn-SBA-15 samples are dominated by the asymmetric Si–O–Si stretch at 1110 cm^{-1} . The symmetric stretch occurs at 809 cm^{-1} , while the band at 456 cm^{-1} is assigned to the Si–O–Si bending mode. The band at 971 cm^{-1} can be assigned to the Si–OH vibration generated by the presence of defect sites. The IR spectra of Sn-SBA-15 samples show a band at 971 cm^{-1} which would correspond to a vibration mode of SiO_4 perturbed by a neighboring SnO_2 or $Sn=O$ (OH) group. According to some authors, this band is observed from the vibration mode of SiO_4 due to the presence of an adjacent $Si-O^{\delta-} \cdots Sn^{\delta+}$ [39]. The presence of this band is generally attributed to the formation of Si–O–M linkages in metallosilicates. Cambor et al. [40] proposed that the band at 960 cm^{-1} is due to the Si–O stretching vibration of Si–OH groups present at defect sites. A band around 580 cm^{-1} was observed in the case of pure SnO_2 (strong) and Sn-impregnated silicalite (weak). The presence of such a vibration in our samples indicates the presence of SnO_2 . Vibrations

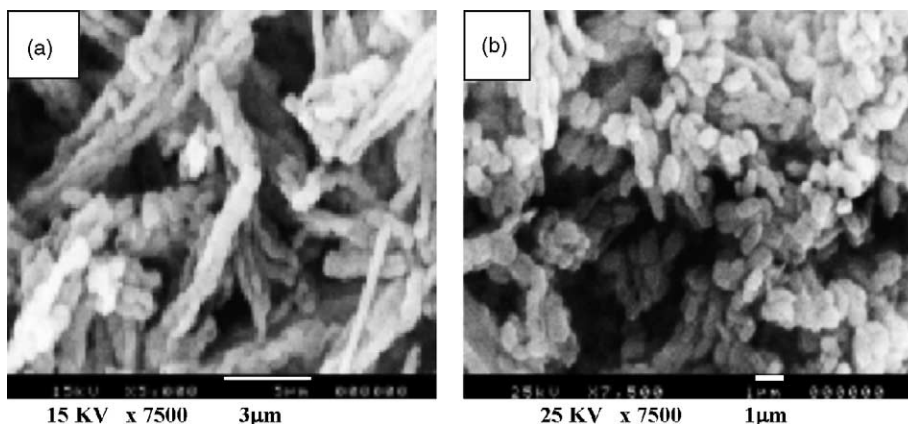


Fig. 3. Scanning electron micrographs of (a) SBA-15 and (b) Sn-SBA-15 (5) samples.

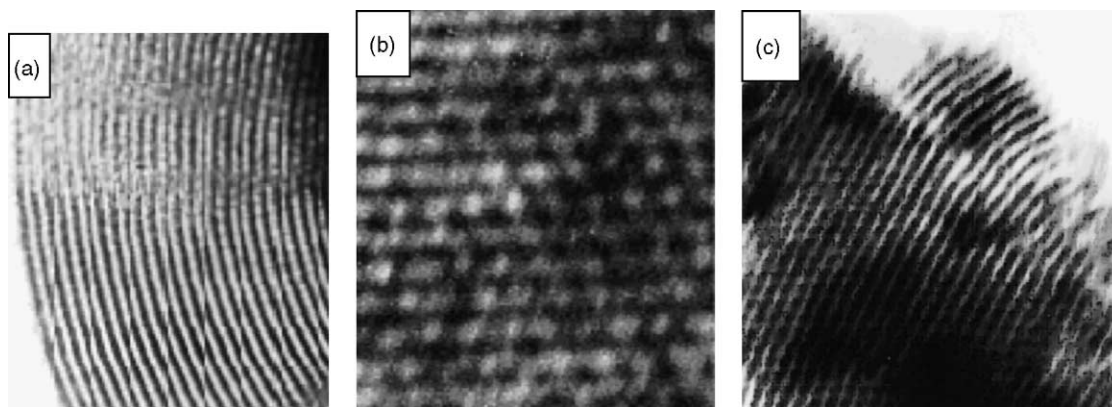


Fig. 4. Transmission electron micrographs of (a) and (b) SBA-15 (c) Sn-SBA-15 (5) samples.

associated with the high surface density of isolated silanols of mesoporous silicates experience a profound change resulting from Sn incorporation. During grafting, these silanols react with the tin chloride precursor.

IR studies in the hydroxyl region ($3800\text{--}3200\text{ cm}^{-1}$) show a decrease in the silanol groups on tin loading (Fig. 6). An intense line of SiOH groups at 3742 cm^{-1} is due to the terminal silanol groups, and a broad absorption at $3400\text{--}3700\text{ cm}^{-1}$ is due to hydrogen bound silanols. The Brönsted acid sites are bridging hydroxyl groups and a band around 3670 cm^{-1} is due to Sn–O–H. The band at 3670 cm^{-1} is also responsible for Brönsted type acidity, as observed in zeolites. The area under the peak per mg of the sample was calculated to quantify the amount of silanol groups present in the samples. A reduction in the intensity shows that less number of silanol

groups are present in the sample loaded with Sn. The integrated intensity of the peak at 3742 cm^{-1} decreases with increase in Sn loading. The presence of silanol OH groups on the wall of SBA-15 which contribute to the micropores in the sample are being used up to react with Sn precursors to form Si–O–Sn–O linkages, which ultimately develop into thin films on the walls of SBA-15.

^{29}Si MAS NMR spectra of the samples are shown in Fig. 7a and b. The broadness of the ^{29}Si signals has been attributed to the large distribution of the T–O–T angle [31]. The broad high field resonance at -110 ppm are due to the Si (OSi) environment (Q^4). The bands at -103 and -113 ppm due to Si (OSi) $_x$ (OH) $_{4-x}$ framework units where $x = 3(Q^3)$ and $x = 4(Q^4)$ respectively. The resonance at -103 ppm arises primarily from Si at defect sites, contain-

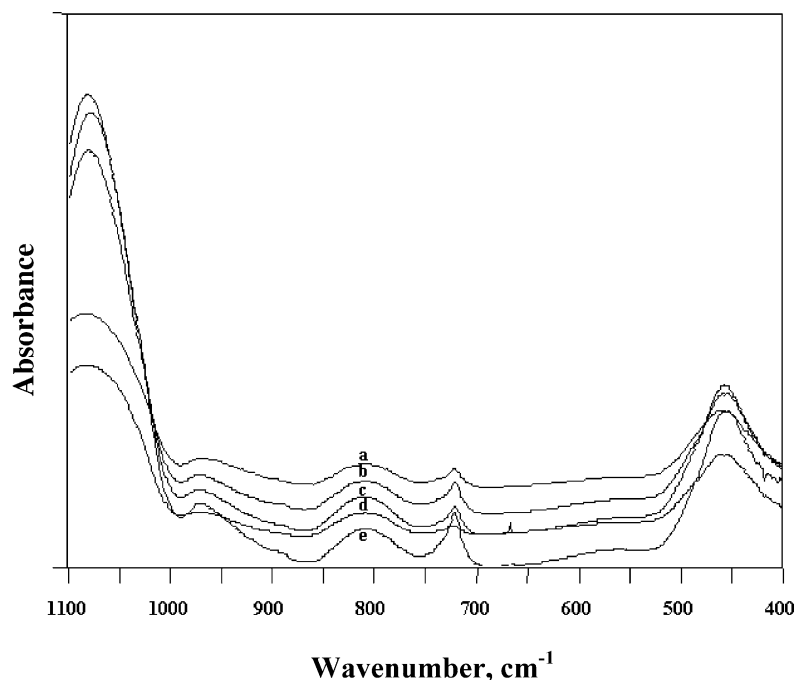


Fig. 5. IR spectra of (a) SBA-15, (b) Sn-SBA-15 (80), (c) Sn-SBA-15 (40), (d) Sn-SBA-15 (20), (e) Sn-SBA-15 (5) samples.

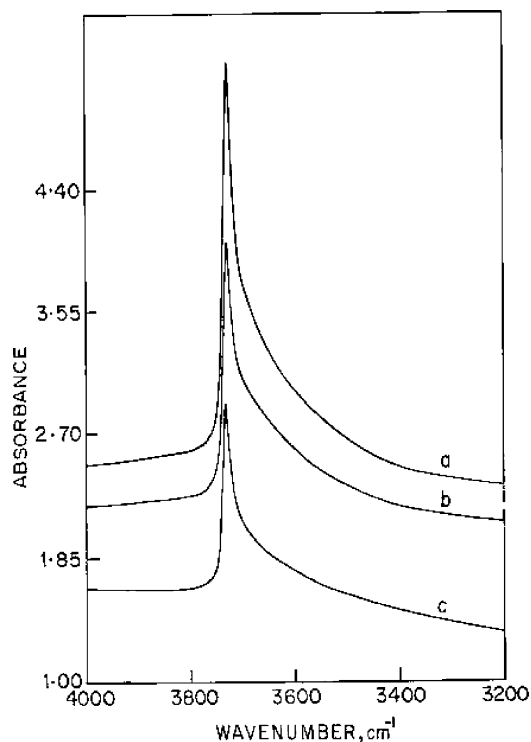


Fig. 6. IR spectra in the hydroxyl region of (a) SBA-15 (b) Sn-SBA-15 (40) and (c) Sn-SBA-15 (5) samples.

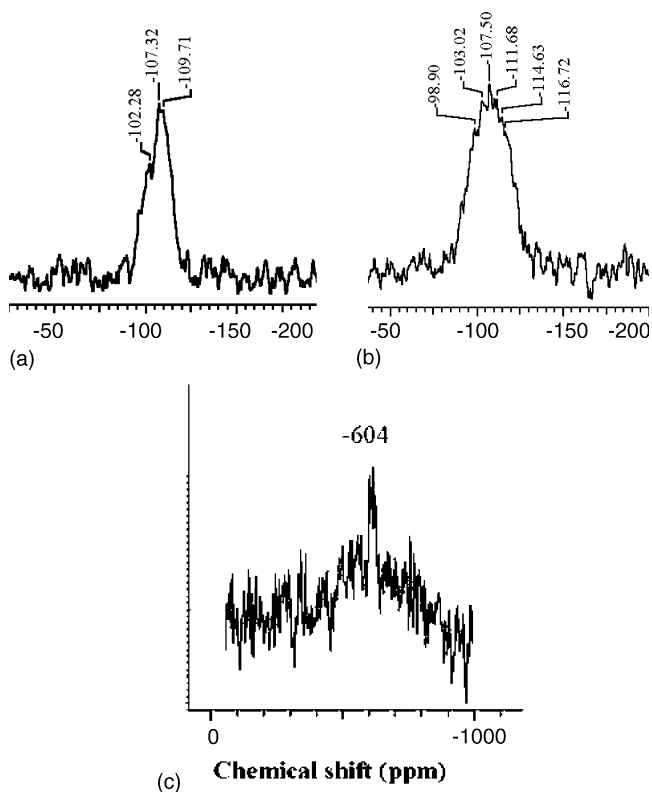


Fig. 7. ²⁹Si MAS NMR spectra of (a) Sn-SBA-15 (80) and (b) Sn-SBA-15 (5) samples and ¹¹⁹Sn static NMR spectra of Sn-SBA-15 (5) sample.

ing Si (OH), Si (OH)₂, and Si–O–R [40,41]. A very weak shoulder at around –116 ppm has been attributed to Si (1Sn) environment.

Though the natural abundance and the magnetogyric ratio of ¹¹⁹Sn are higher than those of ²⁹Si, the detection of Sn in stannosilicates is not easy due to the low concentration, long spin–lattice relaxation times, and, to some extent, the large chemical shift anisotropy (CSA). Nevertheless, an attempt has been made to record the static and MAS spectra of Sn-SBA-15 samples, the results of which are presented in Fig. 7c. The better sensitivity obtained for the samples recorded in the static mode than under MAS conditions is due to the large amount of sample (approximately four times) that could be accommodated in the sample tube (10 mm o.d., ~5 cm length) in the static measurements. For Sn-SBA-15 (input Si/Sn = 5) sample, an isotropic chemical shifts at $\delta = -604$ ppm is observed, which shows the presence of Sn in essentially octahedral environment (Fig. 7). For Sn-impregnated silicalite-1 samples, a similar observation has been made earlier [42].

Mössbauer spectra were obtained on the ¹¹⁹Sn nuclei (on samples with input Si/Sn = 5 and 40). To gather additional information on the possible available sites of tin ions, reduction treatments were also applied on the samples at 670 K (a mild one in CO, and a stronger one in H₂ atmosphere). The spectra are presented in Fig. 8 and the extracted parameters of components are collected in Table 2. The higher tin content allowed collection of spectra at room temperature as well, whereas spectra were recorded only at liquid nitrogen temperature on the lower tin-containing samples.

The dominant component is Sn⁴⁺ ions in each spectrum, accompanied by Sn²⁺ present in various extents (depending on the media of reduction). A further important observation is that the proportion of Sn²⁺ is practically the same in the two hydrogen-treated samples, regardless of their Si/Sn ratios. Thus, it can be suggested that the distribution of tin ions among the possible positions does not depend on the tin content (in a medium Si/Sn region).

For further analysis, it is worth comparing the present spectra with those recorded on microporous MFI, MEL and MTW zeolites [43] and, on another type of mesoporous system, viz., on MCM-41 [44], both type of materials containing tin in isomorphously substituted state. The reduction treatment performed under similar conditions (670 K in H₂) resulted in dominant presence of Sn²⁺ in the 77 K spectra of the tin-zeolites and in those of the Sn-MCM-41 samples, as well. In these substances, more intimate dispersion of tin in the siliceous matrix is assumed, and stabilization of Sn²⁺ was probably more facilitated. In the present Sn-SBA-15 materials, incorporation of tin was less expressed. However, the presence of Sn²⁺ is still noticeable (in the hydrogen-treated samples). Since hydrogen treatment results in Sn⁴⁺ → Sn²⁺ reduction in greater proportion than in carbon monoxide, the role of silanolic groups in formation and stabilization of Sn²⁺ can be proposed. Thus, Sn²⁺ is

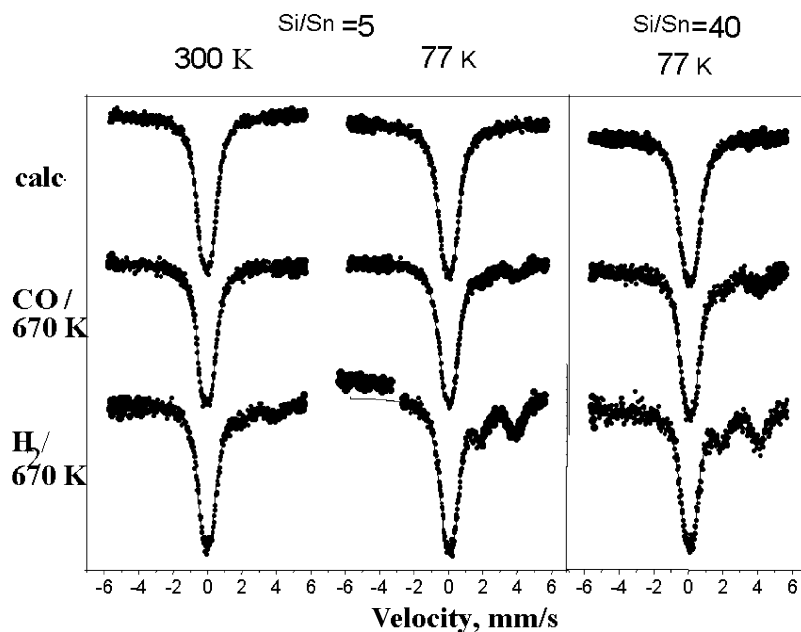


Fig. 8. Mössbauer spectra of a) Sn-SBA-15 (5) and Sn-SBA-15 (40) samples.

Table 2

Mössbauer parameters extracted from the spectra of the Sn-SBA-15 samples

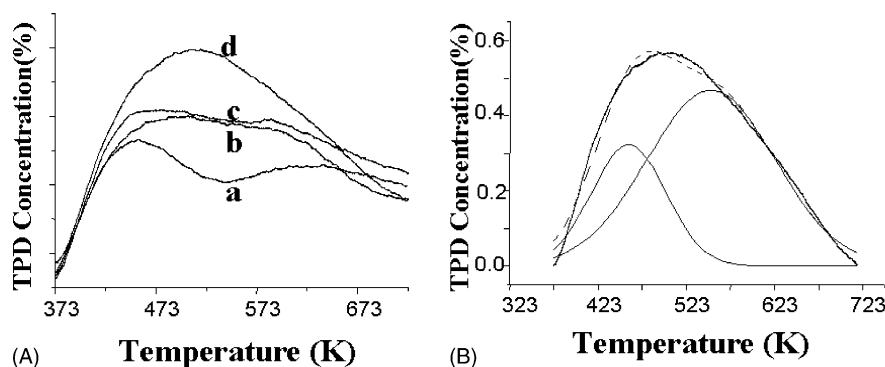
Treatment	Comp	Sample											
		Si/Sn = 5								Si/Sn = 40			
		Meas. temp. (K)											
		300				77				77			
		IS	QS	HW	RI	IS	QS	HW	RI	IS	QS	HW	RI
Calc	Sn ⁴⁺	0.01	0.53	0.86	100	0.04	0.57	0.97	100	0.03	0.58	0.93	100
CO /	Sn ⁴⁺	0.01	0.51	0.79	94	0.05	0.53	0.90	88	0.05	0.54	0.84	84
670 K	Sn ²⁺	2.95	1.80	1.50	6	3.06	2.02	1.01	12	3.11	2.18	1.09	16
H ₂ /	Sn ⁴⁺	0.02	0.49	0.83	91	0.08	0.52	0.85	72	0.06	0.49	0.80	71
670 K	Sn ²⁺	2.97	1.80	0.90	9	2.98	2.05	1.03	28	3.02	2.16	0.92	29

(IS: isomer shift, mm/s, related to SnO₂; QS: quadrupole splitting, mm/s; HW: line-width (full width at half maximum), mm/s; RI: relative percentage of the given component in the spectrum, %).

probably dispersed atomically in the pore wall, whereas Sn⁴⁺ is stabilized in entities of larger size.

Fig. 9 displays the TPD of NH₃ profiles from Sn-SBA-15. The broad desorption pattern indicates a large distribution of different types of acid sites. Deconvolution of the profile

results in two distinct peaks in the range 373–723 K. They can be attributed to two different types of Brønsted acid sites. The desorption peaks are described as follows: (1) the desorption at 373–523 K is assigned to weak acid sites due to surface hydroxyl groups; (2) the peak 523–673 K is attrib-

Fig. 9. (A) TPD of NH₃ of a) SBA-15, b) Sn-SBA-15 (80), c) Sn-SBA-15 (40) d) Sn-SBA-15 (5) samples. (B) Deconvoluted TPD of Sn-SBA-15 (5) sample.

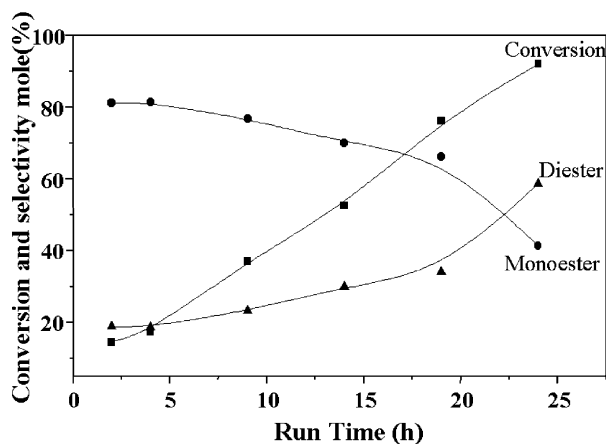


Fig. 11. Effect of reaction time on conversion over calcined Sn-SBA-15 (5) catalyst.

and diester shows the latter being formed at the expense of monoester and points to a consecutive reaction scheme in the presence of Sn-SBA-15 samples. We have studied the transesterification reaction with various alcohols and found that the reaction proceeds well with other alcohols as well (Table 3). It can be inferred that, as the chain length of alcohol increases, the conversion decreases, although the monoester: diester selectivity remains unchanged. Similarly, we observe that transesterification of DEM by benzyl alcohol and allyl alcohol is difficult as compared to that by linear aliphatic alcohols. With benzyl alcohol, the conversion is low, but in the case of allyl alcohol, the conversion is higher but the diester selectivity is low. This means that the reaction is slow, and that a higher temperature may be required to accomplish the reaction in both the cases. The activity of the re-used catalyst is marginally lower than that of the initial one. A very slight decrease in conversion was noticed during recycle (second run) experiments. Successive use of the washed catalyst in batch-wise reaction is possible, as seen from the data given in Table 3.

4. Conclusions

Mesoporous silica SBA-15 molecular sieve has been synthesized and tin was incorporated via incipient-wetness impregnation to produce Sn-SBA-15 samples. Bulk structural characterization techniques (X-ray diffraction and BET) are used to demonstrate that the hexagonal structure is maintained during impregnation procedure. The results given by these two techniques are combined to demonstrate that the Sn species are introduced into the channels of the mesoporous support. In the presence of Sn centers, a noticeable decrease in the specific micropore area, pore volume and diameter is observed, as tin oxide exists as a thin film anchored inside the mesopores of SBA-15. Incorporation of Sn does not affect the original mesopore structure of the parent SBA-15 even at high Sn loading. The FTIR studies in the hydroxyl region show that the abundant surface silanol

groups may be reacting with the Sn precursor. Spectroscopic results reveal that Sn⁴⁺ is present in octahedral coordination. Contributions of tin located in the pore wall (as Sn²⁺) can be distinguished from the signals of oxidic Sn⁴⁺ by decomposing the in situ Mössbauer spectra of the reduced samples. There are probably two types of Sn species in SBA-15, the ratio of which depends on Sn content. The first one is stabilized atomically (well dispersed Si–O–Sn–O–Si-groups) on the walls, which form Sn²⁺ upon reduction treatment (easily reducible from Sn⁴⁺ to Sn²⁺ in presence of –OH groups). The second type is large size entities of Sn⁴⁺(SnO₂) clusters distributed in the external pore structure, which are seen by TEM and are probably agglomerates of smaller crystallites (XRD data). These Sn-SBA-15 samples are effective in catalyzing the transesterification of a diketo ester such as diethyl malonate in the presence of a number of alcohols to give both trans mono as well as diketo esters under mild reaction conditions.

Acknowledgements

The authors are grateful to Dr. P. R. Rajamohanam for NMR spectra and to Ms. Renu Pasricha for TEM and to the Department of Science and Technology, New Delhi, for financial support. Thanks are also due to the Hungarian National Scientific Research Fund for supporting the ¹¹⁹Sn Mössbauer measurements via the OTKA T 032249 Grant.

References

- [1] C.T. Kresge, M.E. Leonowicz, W.J. Roth, J.C. Vartli, J.S. Beck, *Nature* 359 (1992) 710.
- [2] J.S. Beck, J.C. Vartli, W.J. Roth, M.E. Leonowicz, C.T. Kresge, K.D. Schmitt, C.T.-W. Chu, D.H. Olson, E.W. Sheppard, S.B. McCullen, C.J. Higgins, J.L. Schlenker, *J. Am. Chem. Soc.* 114 (1992) 10834.
- [3] A. Sayari, *Chem. Mater.* 8 (1996) 1840.
- [4] A. Corma, *Chem. Rev.* 97 (1997) 2373.
- [5] T. Tatsumi, K.A. Koyano, Y. Tanaka, S. Nakata, *Chem. Lett.* (1997) 469.
- [6] D. Zhao, J. Feng, Q. Huo, N. Molish, G.H. Fredrickson, B.F. Chmelka, G.D. Stucky, *Science* 279 (1998) 548.
- [7] D. Zhao, Q. Huo, J. Feng, B.F. Chmelka, G.D. Stucky, *J. Am. Chem. Soc.* 120 (1998) 6024.
- [8] M. Cheng, Z. Wang, K. Sakurai, F. Komata, T. Saito, T. Komatsu, T. Yashima, *Chem. Lett.* (1999) 131.
- [9] Z. Luan, M. Hartmann, D. Maes, W. Zhao, L. Zhou, Kevan, *Chem. Mater.* 11 (1999) 1621.
- [10] Z. Luan, E.M. Maes, P.A.W. VanderHeide, D. Zhao, R.S. Czernuszewicz, L. Kevan, *Chem. Mater.* 11 (1999) 3680.
- [11] P. Wuy, T. Tatsumi, T. Komatsu, T. Yashima, *Chem. Mater.* 14 (2002) 1657.
- [12] Z. Luan, J.Y. Bae, L. Kevan, *Chem. Mater.* 12 (2000) 3202.
- [13] (a) G. Beaz, in: B.M. Trost, I. Fleming (Eds.), *Comprehensive Organic Synthesis* 6, Pergamon, Oxford, 1991, (P. 323); (b) J. Bertin, H.B. Kagan, J.L. Luche, R. Sitton, *J. Am. Chem. Soc.* 96 (1974) 8113.
- [14] J. Otera, *Chem. Rev.* (Washington, DC) 93 (1993) 1449.
- [15] D. Rehn, I. Ugi, *J. Chem. Res. Synop.* (1977) 119.

- [16] A. Banerjee, S. Senugupta, M.M. Adak, G.C. Banerjee, *J. Org. Chem.* 48 (1983) 3106.
- [17] A. Banerjee, M.M. Adak, S. Das, S. Banerjee, S. Senugupta, *J. Indian Chem. Soc.* 64 (1987) 34.
- [18] R.N. Ram, I. Charles, *Tetrahedron* 53 (1997) 7335.
- [19] A. Rodriguez, M. Nomen, B.W. Spur, J.J. Godfroid, *Tetrahedron Lett.* 39 (1998) 8563.
- [20] G.W. Breton, *J. Org. Chem.* 62 (1997) 8952.
- [21] G.A. Olah, T. Keumi, D. Meidar, *Synthesis* (1978) 929.
- [22] M. Saroja, T.N.B. Kaimal, *Synth. Commun.* 16 (1986) 1423.
- [23] (a) L. Osipow, F.D. Snell, W.C. York, A. Fiuchler, *Ind. Eng. Chem.* 48 (1956) 1459;
(b) J. Otera, T. Yano, A. Kawabata, H. Nozaki, *Tetrahedron Lett.* 27 (1986) 2383;
(c) D. Seebach, E. Hungerbuhler, R. Naef, P. Schnurrenberger, B. Weidmann, M. Zuger, *Synthesis* (1982) 138;
(d) B.S. Balaji, M. Sasidharan, R. Kumar, B. Chanda, *J. Chem. Soc., Chem. Commun.* (1996) 707.
- [24] (a) K. Wakasugi, T. Misaki, K. Yamada, Y. Tanabe, *Tetrahedron Lett.* 41 (2000) 5249;
(b) B.C. Ranu, P. Dutta, A. Sarkar, *J. Org. Chem.* 63 (1998) 6027.
- [25] D.E. Ponde, V.H. Deshpande, V.J. Bulbule, A. Sudalai, A.S. Gajare, *J. Org. Chem.* 63 (1998) 1058.
- [26] G.A. Olah, S.C. Narang, G.F. Salem, B.G. Balaram Gupta, *Synthesis* (1981) 142.
- [27] S.P. Chavan, P.K. Zubaidha, S.W. Dantale, A. Keshavaraja, A.V. Ramaswamy, T. Ravindranathan, *Tetrahedron Lett.* 37 (1996) 233, and 237.
- [28] M. Morey, A. Davidson, H. Eckert, G.D. Stucky, *Chem. Mater.* 8 (1996) 486.
- [29] B.L. Newalkar, J. Olanrewaju, S. Komarneni, *Chem. Mater.* 13 (2000) 552.
- [30] S.J. Gregg, K.S. Sing, *Adsorption, Surface Area and Porosity*, Academic Press, London, 1982.
- [31] K. Miyazawa, S. Inagaki, *Chem. Commun.* (2000) 2121.
- [32] M. Kruk, M. Jaroniec, C.H. Ko, R. Ryoo, *Chem. Mater.* 12 (2000) 1961.
- [33] S. Jun, S.H. Joo, R. Ryoo, M. Kruk, M. Jaroniec, Z. Liu, T. Ohsuna, O. Terasaki, *J. Am. Chem. Soc.* 122 (2000) 10712.
- [34] R. Ryoo, K.C. Hyun, M. Kruk, V. Antochshuk, M. Jaroniec, *J. Phys. Chem. B* 104 (2000) 11465.
- [35] M. Imperor-Clere, A. Davidson, *J. Am. Chem. Soc.* 122 (2000) 11925.
- [36] K. Miyazawa, S. Inagaki, *Chem. Commun.* 21 (2000) 2121.
- [37] M.R. Bhambhani, P.A. Cutting, K.S.W. Sing, D.H. Turk, *J. Colloid Interf. Sci.* 38 (1972) 109.
- [38] N.K. Mal, A.V. Ramaswamy, *J. Mol. Catal.* 105 (1996) 149.
- [39] M. Boccuti, K.M. Rao, A. Zecchina, G. Leofanti, G. Petrini, in: C. Morterra, A. Zecchina, G. Costa (Eds.), *Structure and Reactivity of Surfaces*, Elsevier, Amsterdam, 1989, p. 133.
- [40] M.A. Cambor, A. Corma, J. Perez-Pariente, *J. Chem. Soc. Chem. Commun.* (1993) 147.
- [41] Z. Gabelica, J.L. Juth, *Stud. Surf. Sci. Catal.* 49 A (1989) 421.
- [42] (a) A. Sebald, L.H. Merwin, W.A. Dollase, F. Seifert, *Phys. Chem. Min.* 17 (1990) 9;
(b) N.J. Clayden, C.M. Dobson, A. Fern, *J. Chem. Soc., Dalton Trans.* (1989) 843.
- [43] K. Lázár, A.M. Szeleczky, N.K. Mal, A.V. Ramaswamy, *Zeolites* 19 (1997) 123.
- [44] K. Choudhary, T.K. Das, P.R. Rajmohan, K. Lazar, S. Sivasankar, A.J. Chandwadkar, *J. Catal.* 183 (1999) 281.